

Finite-Size Error in Many-Body Simulations with Long-Range Interactions

Simone Chiesa,^{1,*} David M. Ceperley,^{1,†} Richard M. Martin,^{1,‡} and Markus Holzmann^{2,§}

¹*Department of Physics, University of Illinois Urbana-Champaign, Urbana, Illinois 61801, USA*

²*LPTMC, UMR 7600 of CNRS, Université P. et M. Curie, Paris, France*

(Received 29 April 2006; published 18 August 2006)

We discuss the origin of the finite-size error of the energy in many-body simulation of systems of charged particles and we propose a correction based on the random-phase approximation at long wavelengths. The correction is determined mainly by the collective charge oscillations of the interacting system. Finite-size corrections, both on kinetic and potential energy, can be calculated within a single simulation. Results are presented for the electron gas and silicon.

DOI: [10.1103/PhysRevLett.97.076404](https://doi.org/10.1103/PhysRevLett.97.076404)

PACS numbers: 71.15.Nc, 02.70.Ss

The accurate calculation of properties of systems containing electrons is a very active field of research. Among the possible numerical approaches, quantum Monte Carlo methods are unique in their ability to produce reliable ground state properties at a reasonable computational cost [1]. However, in the simulation of bulk systems, calculations are necessarily performed using a finite number of electrons. In order to reduce the ensuing finite size errors, the system and, hence, the pair interaction are made periodic in a supercell with basis vectors $\{\mathbf{L}_\alpha\}_{\alpha=1,2,3}$. (In the case of a crystal these vectors define a supercell of the unit cell.) This is achieved by using the Fourier components of the interaction at the reciprocal wave vectors of the supercell, i.e., \mathbf{k} such that $\exp(i\mathbf{k} \cdot \mathbf{L}_\alpha) = 1$. Singular long-ranged potentials, such as the Coulomb interaction, are computed by splitting the sum into a portion in real and reciprocal space [2]. Although using the periodized potential reduces the finite-size effects, some error still remains; the one on the energy, for example, often exceeds the statistical noise and other errors characteristic of quantum simulations [3]. Finite-size scaling is possible, but difficult, because the cost of a simulation increases rapidly with the number of particles in the supercell. Here we present an approach that reduces the finite-size errors.

For a supercell of volume Ω containing N electrons, the electron-electron potential energy is conveniently written in Fourier space as

$$V_N = \frac{2\pi e^2}{\Omega} \sum_{\mathbf{k} \neq 0} \frac{1}{k^2} (\rho_{\mathbf{k}} \rho_{-\mathbf{k}} - N), \quad (1)$$

where $\rho_{\mathbf{k}} \equiv \sum_j^N \exp(i\mathbf{k} \cdot \mathbf{r}_j)$ and e is the electron charge. The boundary conditions on the wave function can be chosen as $\Psi(\dots, \mathbf{r}_j + \mathbf{L}_\alpha, \dots) = \exp(i\theta_\alpha) \Psi(\dots, \mathbf{r}_j, \dots)$, where θ_α is the “twist” of the phase in the α th direction. Periodic boundary conditions have $\theta_\alpha = 0$. When there is no long-range order, finite-size errors are reduced by averaging over twists (i.e., k -point sampling or Brillouin zone integration) [4]. This comes at little cost in simulations since the average is also effective in reducing the statistical noise. Even when this is done, the expectation value of

the potential energy remains expressed as a series over \mathbf{k} vectors and is determined by the static structure factor $S_N(\mathbf{k}) = \langle \rho_{\mathbf{k}} \rho_{-\mathbf{k}} \rangle / N$. As the system size increases, the mesh of \mathbf{k} vectors gets finer and the series eventually converges to an integral corresponding to the exact thermodynamic limit.

The error on the potential energy per particle, using a simulation box with N particles, is therefore given by

$$\Delta V_N = \frac{e^2}{4\pi^2} \int \frac{S(\mathbf{k}) - 1}{k^2} d\mathbf{k} - \frac{2\pi e^2}{\Omega} \sum_{\mathbf{k} \neq 0} \frac{S_N(\mathbf{k}) - 1}{k^2}, \quad (2)$$

where $S(\mathbf{k})$ is the structure factor in the thermodynamic limit. The leading order contribution to the error is given by the Madelung constant, v_M , and corresponds to the difference $-e^2 \int_{\mathcal{D}} (2\pi k)^{-2} d\mathbf{k} + 2\pi e^2 \Omega^{-1} \sum_{\mathbf{k} \neq 0} k^{-2}$. It scales as $N^{-1/3}$ because of the omission of the $\mathbf{k} = 0$ contribution from the sum and its value is proportional to $e^2 \int_{\mathcal{D}} (2\pi k)^{-2} d\mathbf{k}$, where \mathcal{D} is a domain of volume $(2\pi)^3/\Omega$.

Although v_M is usually introduced using a real space picture, as the interaction between images, the above perspective can be easily generalized to the next order correction. The remaining part of the error is determined by (i) the substitution of $S(\mathbf{k})$ by the computed $S_N(\mathbf{k})$ and (ii) the discretization of $e^2 \int d\mathbf{k} S(\mathbf{k}) (2\pi k)^{-2}$. The behavior of $S(\mathbf{k})$ at large k is determined by the short range correlation and can be neglected. This is apparent if the potential is decomposed in a short- and long-range part. The long-range part, whose expectation value is affected by the finite size, decays quickly to 0 in reciprocal space so that the behavior of $S(\mathbf{k})$ at large k is irrelevant. Moreover, in the limit $k \rightarrow 0$, one knows that the random-phase approximation becomes exact and describes independent density-fluctuation modes [5]. In the small k region the random-phase approximation suggests

$$S(\mathbf{k}) \simeq S_N(\mathbf{k}) \quad (3)$$

and implies that the leading order contribution to the error comes from point (ii) above. It is an integration error that, analogously to the Madelung constant, comes from the

omission of the $\mathbf{k} = 0$ volume element from the energy sum. Scaling of the finite-size errors is then determined to leading order by this missing contribution, i.e., $e^2 \int_{\mathcal{D}} S(\mathbf{k})(2\pi k)^{-2} d\mathbf{k}$, where \mathcal{D} is a domain centered on $\mathbf{k} = 0$ whose volume equals $(2\pi)^3/\Omega$. This, together with the characteristic quadratic behavior of $S(\mathbf{k})$ for correlated charged systems, leads straightforwardly to the well-known $1/\Omega$ scaling of the error [6]. Thanks to the validity of the random-phase approximation, $S(\mathbf{k})$ can be determined in the small- k region either analytically or from a knowledge of the $S_N(\mathbf{k})$ computed in the simulation. Once $S(\mathbf{k})$ is known, one can accurately compute the correction.

We looked at jellium as a test case to judge to what extent Eq. (3) is verified. Results for $S_N(\mathbf{k})$ computed in variational Monte Carlo simulations at $r_s = 10$ for 12, 24, and 54 particles are shown in Fig. 1. As we increase the number of particles, the grid of k points for which S_N is defined shifts, but the values of S_N fall on a smooth curve, independent of N .

Let us now consider the kinetic energy. It is important to distinguish between the effects due to momentum quantization and long-range correlation. When using a twisted boundary condition $\boldsymbol{\theta}$ in a cubic cell, the kinetic energy is given in terms of the momentum distribution by

$$T_N = \frac{\hbar^2}{2m} \sum_{\mathbf{k}} n_N(\mathbf{k} + \boldsymbol{\theta}/L)(\mathbf{k} + \boldsymbol{\theta}/L)^2, \quad (4)$$

where m is the electron mass. When using a single twist, for example, periodic boundary conditions, the finite-size error is, once again, composed of two contributions: the integration error and the error in approximating the exact momentum distribution, n , with n_N . To better understand the latter point, consider the Fourier transform of the momentum distribution: the one-body density matrix. This is equal to the integral over particle coordinates of

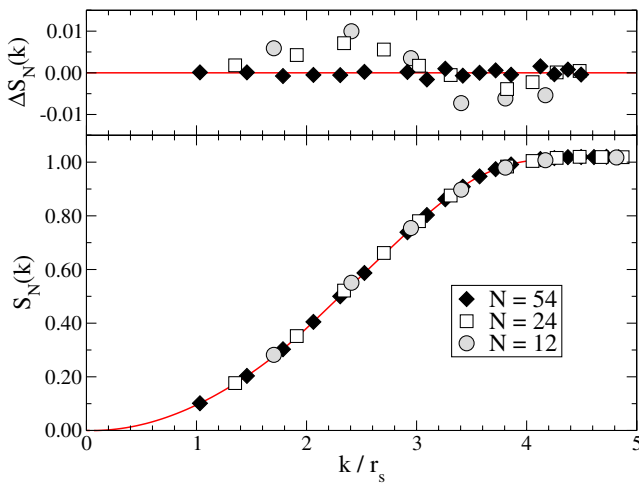


FIG. 1 (color online). Lower panel: static structure factor for the electron gas at $r_s = 10$. Upper panel: $\Delta S_N = S_N(k) - S_{66}(k)$. The difference is computed using a spline function interpolation of S_{66} .

$\Psi^\dagger(\mathbf{r}_1 + \mathbf{r}, \mathbf{r}_2 \dots) \Psi(\mathbf{r}_1, \mathbf{r}_2 \dots)$ and converges to the exact one as soon as the correlation length is less than the size of the simulation box. Under the assumptions of no long-range correlation, this criterion is eventually met so one has $n_N(\mathbf{k}) = n(\mathbf{k})$ and the error comes again from approximating the thermodynamic integral with a sum. At variance with the potential energy case, a change in the twist modifies the grid over which the kinetic energy is computed [see Eq. (4)] so that the error can be made arbitrarily small by increasing the density of twist angles. One can get away with a small number of special k point in the case of semiconductors [7] but a finer grid is needed for a Fermi liquid due to the discontinuity of $n(\mathbf{k})$ at the Fermi surface. In the latter case the occupation of the single-particle states varies with the twist and one can use the grand-canonical ensemble to eliminate this source of error [4].

Consider now the effects due to long-range correlation. In Coulomb systems the interaction causes the wave function to have a charge-charge correlation factor: the Jastrow potential. Within the random-phase approximation the ground state of the system is described by a collection of dressed particles interacting via short range forces and quantized coherent modes, the plasmons. Accordingly, the many-body wave function factorizes as [8]

$$\Psi = \Psi_{\text{s.r.}} \exp \left[-\frac{1}{2\Omega} \sum_{\mathbf{k} \neq 0} u_N(\mathbf{k}) \rho_{\mathbf{k}} \rho_{-\mathbf{k}} \right], \quad (5)$$

where $\Psi_{\text{s.r.}}$ only contains short range correlations and $u_N(\mathbf{k})$ decays quickly to 0 as k increases and diverges as k^{-2} at small k . Because of this divergence, n_N converges very slowly to its thermodynamic value and the average over twists provides only a partial correction. Although one can address the bias on the momentum distribution directly [9], we here employ a different route. Thanks to Green's identity the kinetic energy per particle is written as $T_N = -\hbar^2 \sum_j^N \langle \nabla_j^2 \ln \Psi \rangle / 4mN$ [10] with a contribution coming from the Jastrow potential, T_N^J , given by

$$T_N^J = -\frac{\hbar^2}{4m\Omega} \sum_{\mathbf{k} \neq 0} k^2 u_N(\mathbf{k}) [S_N(\mathbf{k}) - 1]. \quad (6)$$

If $u(\mathbf{k})$ is the optimal Jastrow potential in the thermodynamic limit, the leading order error of T_N^J has a similar mathematical structure to that of Eq. (2):

$$\Delta T_N = \frac{\hbar^2}{4m(2\pi)^3} \int d\mathbf{k} k^2 u(\mathbf{k}) - \frac{\hbar^2}{4m\Omega} \sum_{\mathbf{k} \neq 0} k^2 u_N(\mathbf{k}). \quad (7)$$

It is an integration error provided $u_N(\mathbf{k})$ does not depend on the system size. This must be the case whenever Eq. (3) is satisfied since a difference in $u_N(\mathbf{k})$ would necessarily imply a difference in $S_N(\mathbf{k})$. Under this assumption ΔT_N scales as $1/N$, as a result of the omission of the $\mathbf{k} = 0$ term in Eq. (6).

To compute ΔV_N and ΔT_N we use the Poisson sum formula $\sum_{\mathbf{L}} \tilde{\zeta}(\mathbf{L}) = \Omega^{-1} \sum_{\mathbf{k}} \zeta(\mathbf{k})$, where $\tilde{\zeta}$ and ζ are a

Fourier transform pair. By separating the $\mathbf{L} = 0$ and $\mathbf{k} = 0$ contributions from the two sums we get the expression for the error

$$\frac{1}{(2\pi)^3} \int \zeta(\mathbf{k}) d\mathbf{k} - \sum_{\mathbf{k} \neq 0} \frac{\zeta(\mathbf{k})}{\Omega} = \frac{\zeta(0)}{\Omega} - \sum_{\mathbf{L} \neq 0} \tilde{\zeta}(\mathbf{L}). \quad (8)$$

One sets $\zeta(0)$ equal to the $k = 0$ limit of $2\pi e^2 S(\mathbf{k}) k^{-2}$ or $\hbar^2 k^2 u(\mathbf{k})/4m$ for the leading order correction to the potential and kinetic energy, respectively.

We first apply these corrections to the electron gas for which the small k limits of $S(\mathbf{k})$ and $u(\mathbf{k})$ are known from the random-phase approximation as, respectively, $\hbar k^2/2m\omega_p$ and $4\pi e^2/\hbar\omega_p k^2$, where ω_p is the plasma frequency. In our tests, the wave function had a backflow-Jastrow form [11] and simulations were performed in the grand-canonical ensemble with final energies averaged over twist angles. Thanks to the translational invariance of the Hamiltonian, the wave function factorizes as $\exp(i\boldsymbol{\theta} \sum_j \mathbf{r}_j/L) \Phi$, where Φ , the periodic part, is invariant in a finite pocket of k space around each twist angle. In each pocket the energy dependence on $\boldsymbol{\theta}$ is trivial and one can exploit this fact to reduce the number of twist angles to be the number of inequivalent pockets. This, together with cubic symmetry, drastically reduces the number of needed twist angles to between 20–200 for an unpolarized system with $N \sim 10$ –100. The leading order correction due to long-range correlations to kinetic and potential energy is given by $\Delta V_N = \Delta T_N = \hbar\omega_p(4N)^{-1}$. Corrected and uncorrected variational energies are shown in Fig. 2 for $r_s = 10$. Diffusion Monte Carlo values are uniformly shifted to lower energy by 0.6 mRyd/electron and show similar behavior. One can see that the bias due to the small size

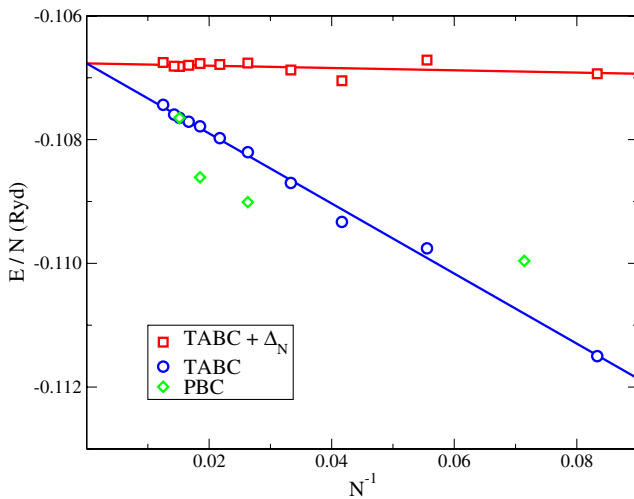


FIG. 2 (color online). Electron gas variational energies per particle at $r_s = 10$ using periodic boundary condition (PBC) and twist-averaged boundary condition (TABC). $\Delta_N \equiv \Delta T_N + \Delta V_N = \hbar\omega_p/2N$ (see text for the definition of ΔT_N and ΔV_N). Error bars are smaller than symbol size.

of the simulation cell is tremendously reduced, so that the $N = 12$ case is already satisfactory.

As a second example we considered the diamond structure of silicon at ambient pressure ($r_s = 2.0$). Calculations were performed using the CASINO [12] code, a Slater-Jastrow wave function, a Hartree-Fock pseudopotential [13,14], and periodic boundary conditions. The orbitals used for the trial function (Hartree-Fock) were from the CRYSTAL98 code [15]. To eliminate the effects of momentum quantization we used a correction based on the density functional eigenvalues of those single-particle states periodic in the simulation cell. Although this is quite common practice, it represents an uncontrolled approximation and results depend weakly on the functional employed (we used the local density approximation). The parameters in the Jastrow potential and a one-body term were optimized. The two-particle Jastrow factor was made up by a spherical short range part and a plane wave expansion including 3 shells of k points for a total of 11 parameters [16]. One needs the plane wave expansion to accurately reproduce the behavior of the optimal Jastrow factor at small k , especially in the case of small simulation cells. To further eliminate errors in the wave function we correct the diffusion Monte Carlo value of $S_N(\mathbf{k})$ by $S_N(\mathbf{k})^{\text{DMC}} - S_N(\mathbf{k})^{\text{VMC}}$ which leads to an estimate correct to second-order in the wave function. The behavior of $S_N(\mathbf{k})$ and $u_N(\mathbf{k})$ for different N is reported in Fig. 3.

For Eq. (8) we assumed $S(\mathbf{k}) = 1 - \exp(-\alpha k^2)$ and $u(\mathbf{k}) = 4\pi a[k^{-2} - (k^2 + a^{-1})^{-1}]$ [17]. When k is expressed in atomic units, the optimal value of α and a

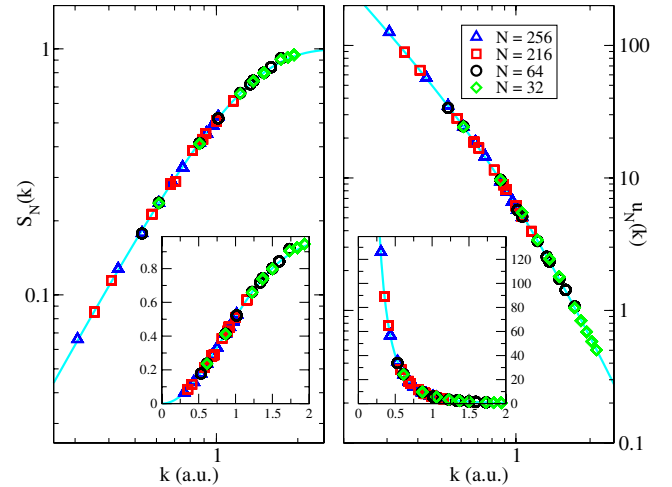


FIG. 3 (color online). Structure factor (left) and Jastrow potential (right) for diamond silicon at ambient pressure. The continuous lines are fit to the data (see text). The Jastrow potential shows a k^{-2} divergence at small k that was not explicitly imposed but obtained through energy variance minimization using the CASINO code. The smallest cell is the conventional fcc cubic cell of diamond (32 electrons). The two intermediate ones are, respectively, $2 \times 2 \times 2$ and $3 \times 3 \times 3$ supercells of the primitive cell (8 electrons). The largest one is a $2 \times 2 \times 2$ supercell of the conventional cubic cell.

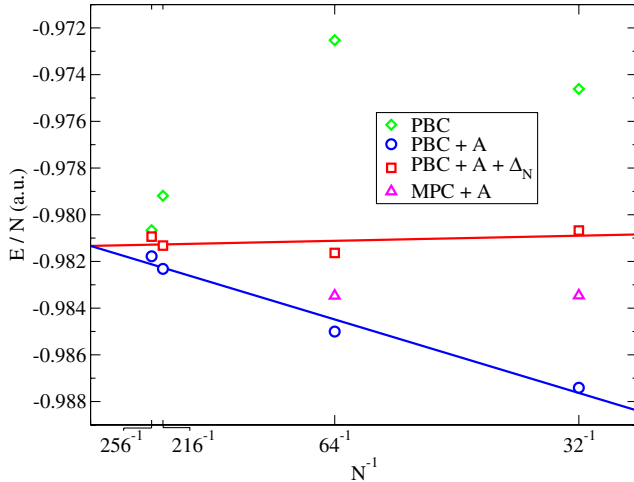


FIG. 4 (color online). Diffusion Monte Carlo energies per electron in diamond silicon at $r_s = 2.0$ using periodic boundary condition (PBC) and the model periodic Coulomb interaction (MPC). “A” corrects for momentum quantization effects (see text). $\Delta_N \equiv \Delta T_N + \Delta V_N$ (see text). Energies and the $S_N(\mathbf{k})$ and $u_N(\mathbf{k})$ used to compute Δ_N are all obtained in simulations with the same number of particles. Error bar on the energies are smaller than the size of the symbols. See caption of Fig. 3 for the description of the cells.

were found to be 0.72 and 1.0, respectively, leading to corrections of $0.13/N$ and $0.092/N$ Hartree per electron for potential and kinetic energy. Results after the two corrections were applied are shown in Fig. 4. Even for the smallest cell (cubic, with 8 Si atoms), the residual finite-size error in the energy is of the order of 1 mHartree/electron (0.1 eV/atom) when compared to the value extrapolated for the infinite size. Two of the calculations were repeated using the model periodic Coulomb (MPC) interaction [18] and results, after momentum quantization effects were removed, are reported in Fig. 4. The MPC interaction removes the bias in $\langle V_N \rangle$ and leads to potential energies in close agreement (within 0.5 mHartree per electron) with those of this Letter. A more subtle point, that lies outside the scope of this work, is to what extent the MPC interaction affects the behavior of $u_N(\mathbf{k})$ and, consequently, the value of ΔT_N .

To conclude, we propose a way to estimate the errors in the potential and kinetic energy under the assumption that the low k behavior of the correlation factor is unchanged upon variation of the simulation cell size. This scheme is suggested by the random-phase approximation that describes independent collective mode in the limit $k \rightarrow 0$. The dominant finite-size errors on potential and kinetic energy are integration errors that can be estimated by using the properties of the charge structure factor and the Jastrow potential at long wavelength. The behavior of these quantities in the small k limit can either be obtained analytically (e.g., for the electron gas) or from results with accurate optimized trial wave functions. This approach can be used

to obtain energies close to the thermodynamic limit without performing a scaling analysis using different sized systems or assuming the finite-size behavior is given by Fermi liquid theory or approximated by density functional theory.

This material is based upon work supported in part by the US Army Research Office under Grant No. DAAD19-02-1-0176. Computational support was provided by the Materials Computational Center (NSF No. DMR-03 25939 ITR), the National Center for Supercomputing Applications at the University of Illinois at Urbana-Champaign, and by CNRS-IDRIS.

*Electronic address: chiesa@uiuc.edu

†Electronic address: ceperley@uiuc.edu

‡Electronic address: rmartin@uiuc.edu

§Electronic address: markus@lptl.jussieu.fr

- [1] W. M. C. Foulkes, L. Mitas, R. J. Needs, and G. Rajagopal, *Rev. Mod. Phys.* **73**, 33 (2001).
- [2] V. Natoli and D. M. Ceperley, *J. Comput. Phys.* **117**, 171 (1995).
- [3] For example, the time-step bias and the fixed node error.
- [4] C. Lin, F. H. Zong, and D. M. Ceperley, *Phys. Rev. E* **64**, 016702 (2001).
- [5] P. Nozieres and D. Pines, *The Theory of Quantum Liquids* (Perseus Books Group, New York, 1999).
- [6] This is only true for those wave functions that properly describe charge fluctuations in Coulomb systems (as is the case in this Letter, thanks to the Jastrow potential). In independent-particle approaches, gapless systems are characterized by $S(\mathbf{k}) \propto k$ at small k and the error is expected to scale as $\Omega^{-2/3}$.
- [7] G. Rajagopal, R. J. Needs, S. Kenny, W. M. C. Foulkes, and A. James, *Phys. Rev. Lett.* **73**, 1959 (1994).
- [8] D. Bohm and D. Pines, *Phys. Rev.* **92**, 609 (1953).
- [9] W. R. Magro and D. M. Ceperley, *Phys. Rev. Lett.* **73**, 826 (1994).
- [10] W. L. McMillan, *Phys. Rev.* **138**, A442 (1965).
- [11] M. Holzmann, D. M. Ceperley, C. Pierleoni, and K. Esler, *Phys. Rev. E* **68**, 046707 (2003).
- [12] R. Needs, M. Towler, N. Drummond, and P. Kent, *CASINO Version 1.7 User Manual* (University of Cambridge, Cambridge, England, 2004).
- [13] J. R. Trail and R. J. Needs, *J. Chem. Phys.* **122**, 174109 (2005).
- [14] J. R. Trail and R. J. Needs, *J. Chem. Phys.* **122**, 014112 (2005).
- [15] V. R. Saunders, R. Dovesi, C. Roetti, M. Causa, N. M. Harrison, R. Orlando, and C. M. Zicovich, *CRYSTAL98 User's Manual* (University of Torino, Torino, Italy, 1998).
- [16] N. D. Drummond, M. D. Towler, and R. J. Needs, *Phys. Rev. B* **70**, 235119 (2004).
- [17] M. S. Becker, A. A. Broyles, and T. Dunn, *Phys. Rev.* **175**, 224 (1968).
- [18] A. J. Williamson, G. Rajagopal, R. J. Needs, L. M. Fraser, W. M. C. Foulkes, Y. Wang, and M. Y. Chou, *Phys. Rev. B* **55**, R4851 (1997).